Proceedings of the ASME 2011 5th International Conference on Energy Sustainability & 9th Fuel Cell Science, Engineering and Technology Conference
ESFuelCell2011
August 7-10, 2011, Washington, DC, USA

ESFuelCell2011-54699

MEMS SENSORS FOR DOWN-HOLE MONITORING OF GEOTHERMAL ENERGY SYSTEMS

Sarah Wodin-Schwartz
UC Berkeley
Berkeley, CA, USA

Matthew W. Chan
UC Berkeley
Berkeley, CA, USA

Kirti Ramesh Mansukhani
UC Berkeley
Berkeley, CA, USA

Albert P. Pisano
UC Berkeley
Berkeley, CA, USA

Debbie G. Senesky
UC Berkeley
Berkeley, CA, USA

ABSTRACT

This paper reviews the limitations in current down-hole monitoring technologies for geothermal energy systems and introduces microelectromechanical systems (MEMS) sensors as a means of optimizing well performance. The use of continuous, real-time, down-hole monitoring can improve geothermal well efficiencies and increase well life. More specifically, monitoring can aid in obtaining accurate temperature and pressure profiles to allow for optimized well reinjection and energy extraction. A variety of materials used in the fabrication of MEMS sensors have been tested in an experimental geothermal environment (critical-point water) and exposed for up to 100 hours. The results obtained from the exposure testing support the use of harsh environment materials to create a suite of sensors that can be permanently located down-hole. MEMS-based temperature and pressure sensors using a harsh environment materials platform are currently in the design phase for down-hole monitoring. In addition to designing harsh environment sensors that can reliably monitor down-hole conditions, suitable packaging must be considered. One vision is to mount the sensors to the well casings through the use of new bonding technologies.

INTRODUCTION

The advancement of renewable energy technology is critical due to unstable energy sources and the expected increase (by a factor of two) in electricity demand by 2030 [1]. The improvement of hydrothermal systems and the development of enhanced geothermal systems (EGS) has the potential to provide at least 200,000 EJ at around 100,000 MWe, of stable, base load energy, in as little as 50 years [2]. However, complex geochemical and geophysical properties of the subsurface environment make engineering reservoirs challenging. Current technology utilizes either surface measurements to develop thermal and geophysical profiles or down-hole sensors mounted to large testing apparati which require expensive cabling and are designed for short duration well monitoring. The accuracy of these profiles can be enhanced by subsurface data logging, which will provide data to optimize drill site locating and increase the lifetime of geothermal reservoirs.

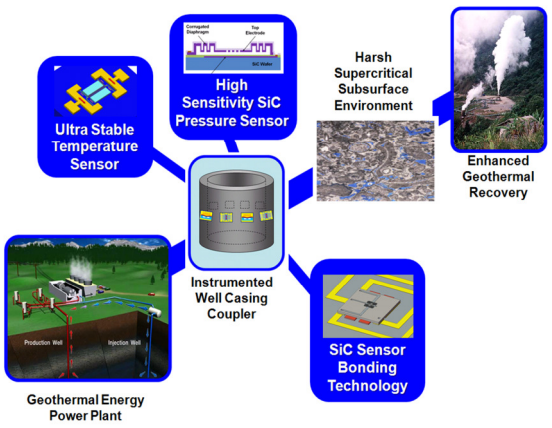

Figure 1- Graphic detailing the implementation of harsh environment MEMS sensors in down-hole, geothermal systems.

Microelectromechanical systems (MEMS) sensors and packaging are nearly planar and millimeters in size. This size reduction allows for sensor mounting to well casings for permanent monitoring and easier well insertion and removal

from wells for temporary monitoring without the well obstruction experienced with current technologies. However, traditional MEMS sensors are limited to temperatures below 300°C due to thermal limitations in commonly used semiconductor materials (e.g. silicon). Harsh environment MEMS sensors, fabricated from ceramic materials such as silicon carbide (SiC) and sapphire (Al_2O_3) offer an alternative to traditional semiconductor materials due to their chemical robustness and high-temperature operation. In addition, macro-scale sensors that are currently used by the geothermal industry require costly packaging (e.g. flasking) to protect the sensors and electronics from its operation environment. Furthermore, wireless technologies can be utilized for signal transmission from MEMS sensors in harsh locations to down-hole data acquisition logging units in more protected down-hole locations. This type of logging unit could either be removed for data retrieval or used to transmit data to an above ground data station.

In addition to the challenges of fabricating robust sensors for harsh geothermal environments, adhering sensors to casing components for well monitoring with permanent bonding technology is difficult due to mismatched coefficients of thermal expansion of the steel well casings and the ceramic SiC sensor substrate material. Many attachment techniques are investigated for down-hole use.

CURRENT GEOTHERMAL LIMITATIONS

Hydrothermal and EGS systems have few technological barriers to overcome to achieve operational status. However, system optimization to enhance well operation and reduce exploratory well costs requires more advanced feedback systems utilizing harsh environment sensors. Increased knowledge of down-hole conditions including precise well temperatures, pressures, chemical composition, depth, flow rates and other physical parameters are useful data for power plant operators. For example, an understanding of the physical and chemical conditions would improve well operators abilities to determine optimized reflow rates, energy extraction rates and well lifetime expectancy. This would allow for the generation of improved geothermal modeling which would both increase the life of current wells and give more accurate lifetime information for potential well sites. In addition, appropriate safety precautions (or predictive measures) can be taken when approaching anomalies in the borehole. For example, operators need to plan for sudden drops in pressure in the borehole due to wash-outs or jumps in pressure due to gas/fluid pockets of reservoir [3].

Current geothermal sensors can be broken down into two categories, exploratory tools for site planning and well monitoring tools. Each of which has both surface and sub-surface tools. Surface exploratory tools are focused around locating geological indicators such as carbonates (sinter and tufa), clays or sulfates that result from hydrothermal alteration, and thermal anomalies [4], such as surface exhaust vents and hot springs. These indicators can be discovered using direct surface sample analysis or through the use of air and space craft imagery. Research in the use of infrared imagery has given promising results in lowering exploratory well location identification costs [4]. Initial well identification is an important part of the exploratory process as it shows where test wells should be constructed. However, surface exploratory sensing does not give complete evidence that a given location is ideal for geothermal energy extraction. Once a potential well site has been identified, down-hole sub-surface exploratory tools are needed to determine the wells' viability.

Current sub-surface exploratory tools are very large and expensive. Subsurface tools are used to determine rock thicknesses, porosities, fracture patterns, pressure, temperature, salinity and steam quality. In addition, direction and inclination sensors are also important for drilling navigation especially for very deep and deviated (non-vertical) holes. This data is acquired using thermal, magnetic, electrical, radiation and acoustic sensors [5]. All of these properties are collected to generate a subsurface map to determine the ideal locations to drill wells for power generation.

Usually all of these tools are combined into a single multi-tool that is sent down-hole for temporary well state analysis. All of these probes are macro-scale and require active cooling or expensive Dewar flask sealing while down-hole due to the harsh environmental constraints. These tools are very long, up to 5' in length, and are only capable of 4-6 hours of down-hole operation [6].

Currently, well monitoring sensors are located at the surface level. While there exsists down-hole sensing tools used during well operation to monitor well performance, these devices are limited to short duration uses and reduce well efficiency. While some monitoring sensor systems claim to be permanent down-hole fixtures, they are currently either limited by temperature, exposure time, or both. Newer fiber-optic technologies are currently under investigation for down-hole applications, however, the leading cable is currently limited to 300°C and must run the full length of the well to transmit optical pulses [7,8]. The surface well monitoring sensors currently monitor properties including flow rate, surface water temperature, surface water pressure and water chemical composition. This does not give the most immediate or accurate information as to the conditions down-hole.

While all of this data is valuable, an understanding of the down-hole conditions is necessary to generate a full geophysical map to decrease the cost of well exploration and improve operational well efficiency.

MEMS HARSH ENVIRONMENT MATERIALS

To explore the development of a robust sensor platform for harsh geothermal conditions, SiC, Al_2O_3, and Si (as a control), were all selected as potential sensor substrates or encapsulation materials. These materials have been shown to survive high temperature testing and most of them are very stable compounds, see Table 1.

Property	Al_2O_3	Silicon Carbide 3C-SiC (6H-SiC)	Silicon	Diamond
Melting Point (°C)	2030	2830 (2830)(sublimes)	1420	4000 (p.c.)
Energy Gap (eV)	n/a	2.4(3.0)	1.12	5.6
Critical Field (x10^6V/cm)	0.48	2.0 (2.5)	0.25	5
Thermal Conductivity (W/cm-K)	0.42	5.0 (5.0)	1.5	20
Young's Modulus (GPa)	470	450 (450)	190	1035
Acoustic Velocity (x10^3 m/s)	11.1	11.9 (11.9)	9.1	17.2
Yield Strength (GPa)	2.25	21 (21)	7	53
Coeff. Of Thermal Expansion (°C x 10^6)	7.7	3.0 (4.5)	2.6	0.8
Chemical Stability	Excellent	Excellent	Fair	Fair

Table 1- Materials properties of high-temperature materials used in harsh environment sensor fabrication.

The weight of each sample was measured before and after exposure testing in water at its critical point (22 MPa at 374°C). The critical point was chosen as geothermal wells have a range of water conditions and as this point is unstable, the sensors would experience super-critical, liquid, and vapor phases. Tests ranging from 1 to 100 hours were conducted in Tuttle pressure vessels as shown in Figure 2.

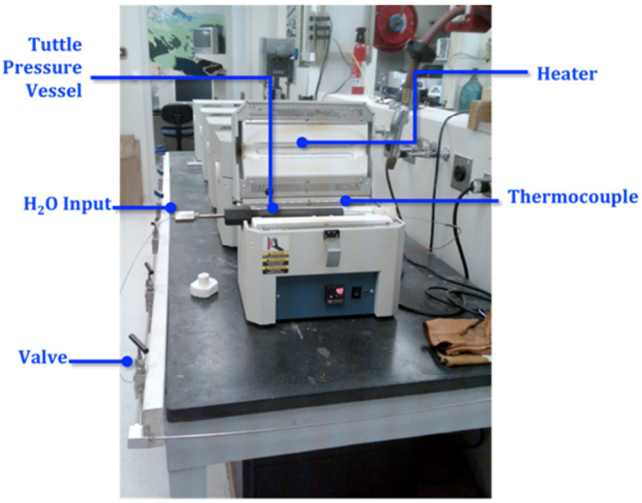

Figure 2- Tuttle pressure vessel testing apparatus for exposure testing.

Significant weight loss of the Si was observed while the weight changes of the SiC and Al_2O_3 were minimal, on the order of 5 µg. The results for these tests are shown in Figure 3. There is a nearly linear mass loss trend for the Si based samples with time. These results indicate that specialized harsh environment materials are necessary for directly exposed down-hole sensors. Both the SiC and Al_2O_3 appear to be physically unaffected by the harsh environment and are likely suitable for sensing applications.

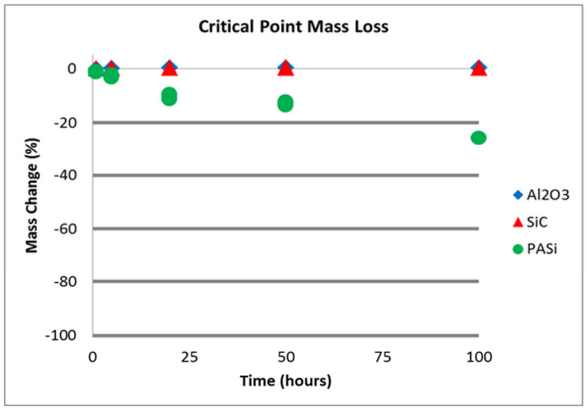

Figure 3- Weight loss for Al_2O_3 and SiC substrates and a Si based sample from 1 to 100 hours exposure in water at its critical point.

CAPACITIVE SENSING

There is a tradeoff between sensor footprint size and capacitive resolution when designing MEMS sensors. Commercial capacitance sensors generally have a nominal capacitance in hundreds of picofarads and operate with a few hundred pico-farad range [9, 10]. However, MEMS capacitive sensors often have capacitive readouts that are smaller, in the atto- to femto- farad range [11-13]. The Irvine Sensors MS3110 capacitance to voltage converter, designed for MEMS capacitive sensor readout, has a noise floor of 4af/rtHz [14] which sets a minimum possible capacitance resolution. These two capacitance value extremes leave a large window in which to design MEMS sensors. However, this range is greatly reduced when we consider that this variable capacitance is desired for use within a resonating LCR circuit for RF transmission.

RF signal transmission operates within the frequency bands of MHz to lower GHz. The resonance of an LCR circuit is determined by both the capacitor and the inductor. At resonance, the capacitor reactance X_C and inductor reactance X_L must be equal. Circuit resonance occurs when electrical impedance is minimized. Electrical impedance, Z, is defined by:

$$Z = \sqrt{Z^2 + (X_C - X_L)^2}. \quad (1)$$

At resonance,

$$X_L = \omega L = X_C = \frac{1}{\omega C} \quad (2)$$

$$C = \frac{1}{\omega^2 L} \quad (3)$$

where C is the capacitance, L is the inductance and ω is the circuits resonance frequency.

The desired capacitance range is in part determined by the inductors that can be fabricated using micro-scale techniques. Most MEMS scale on-chip inductors have values on the order

of nano-Henry's [15-17], resulting in a capacitor range of pico-Farad's. However, recently inductors in the range of µHenry's have been fabricated using microfabrication techniques [18]. Using inductors in the µHenry range allows for the use of capacitors in the femto-farad range while maintaining a GHz band.

On the MEMS scale, capitalizing on the coefficient of thermal expansion (CTE) mismatch for different materials is an effective method for measuring ambient temperatures. A CTE mismatch is utilized in sensor design to move patterned sensor features relative to other features as shown in Figure 4. This relative motion can be measured using physical effects such as frequency shifts of resonators, resistance change due to induced stress in piezoresistive materials, capacitance changes from moving parallel plate systems or other phenomenon.

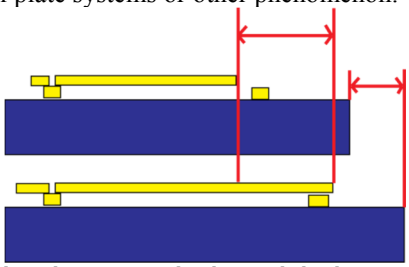

Figure 4- Both substrate and released device expand, but CTE mismatch makes the device expand more in this case.

The development of low power, passive devices is advantageous in this situation as these sensors will be used in harsh environments. This makes a capacitive sensor read out attractive. The variable capacitor can be connected in a circuit with an inductor to make an LC circuit whose resonance frequency can be determined using an external radio frequency (RF) system. This would result in a sensor that needs little to no power provided at the measurement location.

Traditionally capacitive MEMS sensors are fabricated with either inter-digitated comb fingers or parallel plates. Capacitors operate based on the equation $C = \frac{\varepsilon A}{d}$ were Ɛ is the dielectric constant of the medium between the two plates, A is the overlapping area and d is the distance between the two plates. In an in-plane system the motion between the two plates is ideally either perpendicular or parallel relative to each other for parallel plates and comb fingers respectively. These relative motions can be seen in Figure 5.

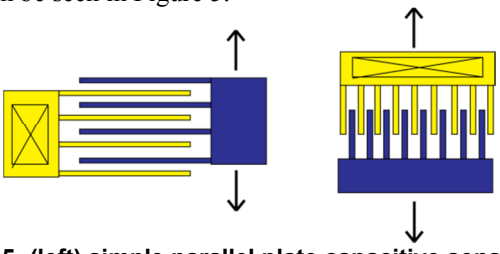

Figure 5- (left) simple parallel plate capacitive sensor. (Right) simple inter-digitated comb fingers capacitive sensor.

TEMPERATURE SENSOR DESIGN

Geothermal environments have varied average temperatures from well to well based on many factors including well depth, mineral content, water pressure and other environmental parameters. For this sensor design an average well temperature of 374°C is used as it is the temperature of waters' critical point with 22 MPa pressure. A temperature range of ±50°C was used to give a reasonable temperature range to monitor long term well temperatures and for use in a wide variety of well conditions. The sensor design is easily tailored to a new temperature range if deemed necessary.

A clamped-clamped beam was chosen for the base mechanical design as described in Figure 6. This structure behaves as a controlled buckling beam. While pure buckling of an isotropic beam is unstable and directionally unpredictable, a bimorph structure on each end guides the beams buckling to give a controlled motion.

Either parallel plates or comb fingers can be attached to this structure to generate the capacitive readout. Finite element analysis can be conducted to determine the beam deformation due to thermal loads (Figure 7). Basic geometric models can be generated using the bimorph equation, however for more complicated geometries, a finite element modeling tool such as ANSYS is beneficial to optimize the structures parameters. Theoretical capacitive values can then be determined based on the modeled deformations and the other structure parameters using the capacitance equation.

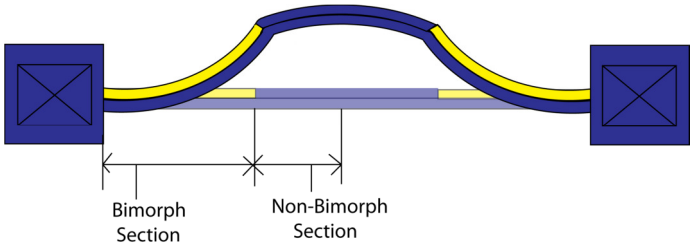

Figure 6- Double bimorph connected by single beam deformed due to heating.

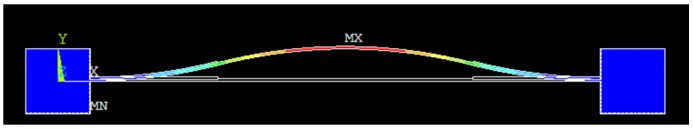

Figure 7- Results of ANSYS simulation showing relative deformation in the Y direction of a connected double bimorph structure.

The buckling instability can be seen as the ratio of bimorph to non-bimorph section approaches 1. In Figure 8, a full double bimorph beam with no non-bimorph section is shown deflecting with temperature. The instability due to the bucking is more dramatic. As the system motion is dominated by the linear thermal expansion, the length ratio of the bimorph to non-bimorph section has a minimal effect on the overall system displacement once the beam has buckled. This length ratio also

has a minimal effect on the linearity of the structures displacement between 250°C to 450°C. The overall length of the structure (anchor to anchor distance) can be increased to improve orthogonal displacement. However, the longer the overall structure, the larger the mass of the system which makes the sensor less shock resistant.

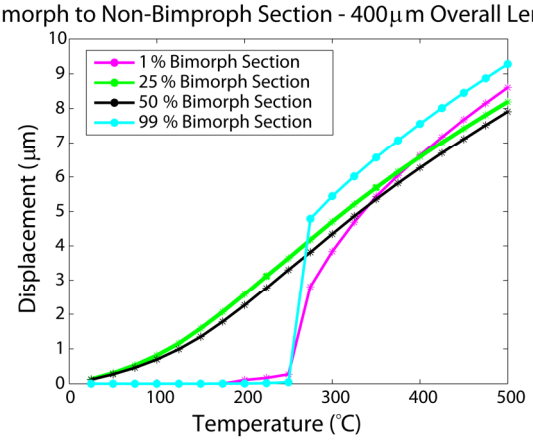

Figure 8- Maximum transverse displacement of the center of the 400 μm double bimorph. The 99% line (cyan) and the 1% (magenta) line show the beam buckling more dramatically than the structures with a smaller bimorph to non-bimorph ratio.

PRESSURE SENSOR DESIGN

Monitoring well pressure during geothermal energy production is important for safety, optimization and lifecycle management. Pressure is primarily used to detect fluid-steam interfaces [19]. Currently, the technology for such sensors is limited to macro-scale quartz crystal or strain gauge type sensors [20]. These sensors require power and electronics at the senor location which is not ideal for this harsh environment.

This work proposes a MEMS-scale sensor that utilizes capacitive sensing to measure pressure. The edge-clamped, SiC diaphragm that deflects toward the base of a sealed cavity under the application of external pressure is shown in Figure 9. An electrode connected to the diaphragm and one in the base combine to form a parallel-plate capacitor. As gap between the electrodes decreases under applied pressure, the capacitance changes. Various diaphragms with different shapes (square, circular) and cross-sections (corrugated, flat) can be designed depending on the application requirements.

Due to the inverse relationship between the gap and capacitance, nonlinearity is one of the primary limitations of capacitive pressure sensors. The design therefore utilizes a touch mode operation which has been shown to achieve good linearity, large operating pressure range and the ability to withstand higher burst pressures hence providing overload protection at output [21, 22]. Operation in "touch mode" allows the diaphragm to contact the base of the cavity which is coated with a thin dielectric layer to prevent a short circuit between the top and bottom electrodes. The contact area increases with pressure, thereby increasing the capacitance. The area-induced capacitance, the linear component shown in Equation 4, rapidly dominates over the gap-induced capacitance. The linear behavior in the touch mode regime gives the sensor a higher sensitivity than when operated in normal, non-zero gap, mode. The load-deflection equation for corrugated diaphragms [23] is as follows:

$$\frac{Pa^4}{Eh^4} = A_P \frac{y}{h} + B_P \frac{y^3}{h^3} \quad (4)$$

Where P is the differential pressure, a is the diaphragm radius, h is the thickness, y is the vertical displacement, E is Young's modulus and A_p and B_p are dimensionless stiffness coefficients.

In addition, corrugated diaphragms, shown in Figure 10, have been used in MEMS applications to enable operation at larger displacements and have a longer linear travel as compared to a flat diaphragm.

The load-area relationship can either be determined by modeling or using numerical techniques [22, 23]. The total capacitance-pressure relationship can therefore be determined for a given diaphragm over the operating pressure range. At present, the proposed design is being optimized for the given pressures up to 220 bar.

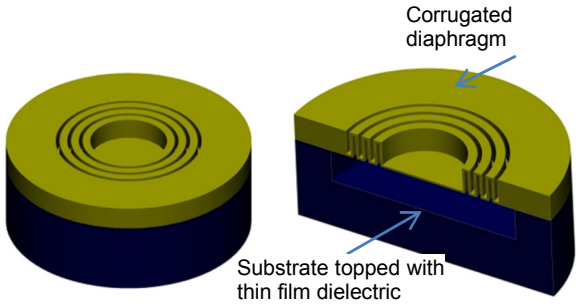

Figure 9-Schematic image of proposed design for capacitive pressure sensor.

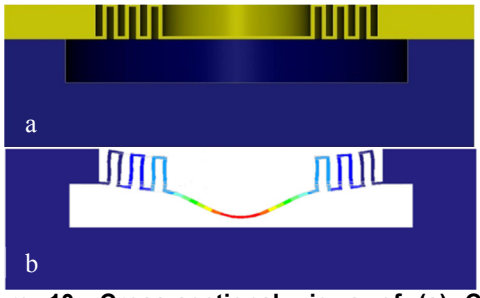

Figure 10- Cross-sectional views of (a) Corrugated diaphragm (b) Deformed corrugated diaphragm under external pressure simulated in ProMechanica.

HARSH ENVIRONMENT BONDING

Implementation of MEMS sensors for down-hole monitoring requires a robust bonding system. Bonding and testing of both silicon and aluminum nitride (AlN) resonant MEMS strain gauges to 1095-steel has been demonstrated using a lead-free low-temperature solder [24, 25]. However,

with the harsh environments encountered in geothermal operations, solders are unsuitable with their low melting temperatures, typically below 350°C. Instead, because of the higher bonding temperature required, brazing methods and other high-temperature joining technologies are necessary. Furthermore, the numerous types of substrate materials used in MEMS require bonding technologies that are tailored to ceramics and other non-metals.

Typical brazing processes take place at temperatures higher than the operational temperature of the components being bonded, which can lead to a major complication with high-temperature bonding. The higher brazing temperature is required to avoid creep in the bond; however, it introduces greater CTE mismatch. Typical substrates such as silicon, silicon carbide, silicon nitride, aluminum nitride, and aluminum oxide have drastically different coefficients of thermal expansion from the well casing steels used in geothermal applications. Upon cooling, the large thermally induced strains can cause delamination of the metal used for bonding, cracking of the MEMS substrate, and mechanical failure of the bond.

Some methods have been presented to overcome this problem. One is simply to choose braze alloys that have lower melting points. The tradeoff with this approach is that although lesser thermal-strains are induced, maximum service temperature of the sensor is inherently reduced.

As important as heating for bonding may be, the cooling process used post-bond is just as vital. Depending on the metallurgy used for bonding, an optimal cooling scheme may be utilized, as demonstrated with gallium arsenide substrate bonding by Chandran et al [26]. Using a carefully controlled cooling process, the mechanical creep in the bond-layer can be used to absorb the thermal strains induced upon cooling.

A different approach that enables high-temperature ceramic-to-metal brazing, presented by Zhong, uses the use of metal intermediary layers, such as tungsten/nickel to absorb and accommodate for the thermally induced strains [27]. The thicknesses of these strain-absorbing layers are quite large for typical MEMS bonding applications and the strain-transfer characteristics of this bonding approach have yet to be determined.

Another viable option for MEMS bonding that alleviates CTE mismatch utilizes a technique known as Transient Liquid Phase (TLP) bonding, sometimes referred to as the Solid Liquid Inter-Diffusion (SLID) process or diffusion brazing. This bonding method utilizes two metals, one having a low melting point and the other having a high melting point. These metals are deposited on the MEMS substrate in layers using standard microfabrication techniques. During heating, the low melting point metal liquefies and solid-liquid diffusion takes place forming alloys that have a melting point somewhere between the two original metals [28, 29]. A generic version of this process is shown in Figure 11. Some common examples of metals used are Au-Sn, Ag-Sn, Ti-Ni and Au-In. The metallurgy and thickness of the layers deposited will depend upon the substrate type and the specific sensor application. Using this method, it is possible to join MEMS sensors at temperatures below final service temperature, thus reducing some thermal strain.

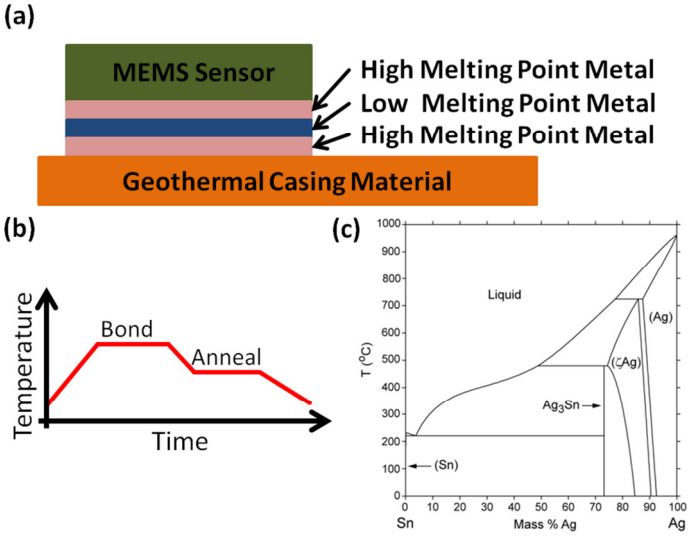

Figure 11- A typical bonding material stack for TLP bonding of a MEMS Sensor to a geothermal casing (a). The heating profile (b) is used to melt the low melting point alloy and cause solid-liquid diffusion, which develops alloys with increased melting point (c). The Sn-Ag phase diagram taken from the NIST standards library is shown to exemplify a high-low melting point combination. Annealing further enhances the formation of these intermetallics [30].

For the bonding of MEMS on ceramic substrates, super alloys may be used to match the coefficient of thermal expansion of the ceramic. A partial TLP bonding process has been utilized by Park to bond Si_3N_4 to Inconel 718 with Ti-Cu, Ti-Ni, and Ti-Cu-Ni layers [31]. For such an application, very high bonding temperatures can be achieved without great CTE mismatch between the Inconel and Si_3N_4.

These different approaches to bonding MEMS sensors to geothermal casings provide production-worthy methods of implementing miniature MEMS sensors for geothermal monitoring. However, challenges in creating a fully packaged system still remain.

CONCLUSIONS

Using MEMS sensors for down-hole geothermal monitoring will decrease the costs associated with well exploration and will allow for well production optimization. Down-hole pressure and temperature sensors, as well as other future sensors, will collect data to generate underground maps which can be used to create more advanced geothermal computer models. This will help with both current and future well sites.

The necessity for harsh environment materials has been proven with the exposure testing. Further analysis is necessary to determine which of the SiC and Al_2O_3 materials is best for substrate and encapsulation purposes.

Initial temperature and pressure sensors have been designed for down-hole applications. Fabrication for proof of

concept must be conducted. MEMS sensor bonding has been investigated. Many potential techniques exist for this technology. These must be tested to determine the best bonding method.

ACKNOWLEDGMENTS

The authors would like to thank the Department of Energy's Enhanced Geothermal Systems program for funding this research (grant # DE-FOA-0000075).

REFERENCES

[1] D. Chandrasekharam and J. Bundschuh, *Low-Enthalpy Geothermal Resources for Power Generation*, CRC Press, London, UK, 2008.

[2] *The Future of Geothermal Energy: Impact of Enhanced Geothermal Systems (EGS) on the United States in the 21st Century,* (Massachusetts Institute of Technology, 2006). http://www1.eere.energy.gov/geothermal/future_geothermal.html.

[3] J. Finger and D. Blankenship, *Handbook of Best Practices for Geothermal Drilling,* SANDIA REPORT SAND2010-6048, December 2010, http://www1.eere.energy.gov/geothermal/pdfs/drillinghandbook.pdf

[4] Calvin, Wendy M. and Coolbaugh, Mark and Kratt, Chris and Vaughan, R. Greg, *Application of Remote Sensing Technology to Geothermal Exploration*, Great Basin Center for Geothermal Energy (GBCGE) and the Department of Geological Sciences, 2005, http://www.unr.edu/geothermal/pdffiles/CalvinGSN05.pdf

[5] Candela, Lucilia, *Advances in Subsurface Pollution of Porous Media: Indicators, Processes and Modeling,* CRC Press, 2008

[6] K10 Geothermal PTS –SRO Instrument Operation & Service Manual, Kuster Company, Long Beach, Ca, 2010

[7] Jaaskelainen, Mikko, *Distributed Temperature Sensing (DTS) in Geothermal Energy Applications,* Sensors Magazine, 2009

[8] Qorex: Fiber Optic Monitoring, MICA Controls LTD, http://micacontrols.com/fibre-optic.html

[9] Yurish, S. Y., *Universal Capacitive Sensors and Transducers Interface*, Eurosensors XXII Conference, pp. 441-444, 2009.

[10] Ruff, M., H. Mitlehner, and R. Helbig, *SiC Devices: Physics and Numerical Simulation,* IEEE Transactions on Electron Devices, 41 (6), 1994.

[11] Warren, C. G., *Polymer-Ceramic MEMS Bimorphs as Thermal Infrared Sensors*, PhD Thesis, UC Berkeley, p. 105, 2010.

[12] Azevedo, R. G., *Silicon Carbide Micro-Extensometers for Harsh Environments*, PhD Thesis, UC Berkeley, p. 201, 2007.

[13] Jamshidi, B., *Poly-Crystalline Silicon Carbide Passivated Capacitive MEMS Strain Gauge for Harsh Environments*, PhD Thesis, UC Berkeley, p. 157, 2008.

[14] Sensors, I., MS3110 Universal Capacitive Readout IC, 2004.

[15] Dai, C.-L., J.-Y. Hong, and M.-C. Liu, *High Q-factor CMOS-MEMS inductor*, DTIP of MEMS and MOEMS, 2008.

[16] Li, L., and D. Uttamchandani, *Monolithic RF MEMS inductor using silicon MEMS foundry process*, Micro and Nano Letters, 1 (1), 5-8, 2006.

[17] Tseng, S.-H., Y.-J. Hung, Y.-Z. Juang, and M. S.-C. Lu, *A 5.8-GHz VCO with CMOS-compatible MEMS inductors*, Sensors and Actuators, 139, 187-193, 2007.

[18] Wang, J. J., *Adjustable, Integrated Inductors and Transformers*, INDUCTICA Conference, 2010.

[19] R. A. Normann, B. J. Livesay, *Geothermal High Temperature Instrumentation Applications,*

[20] Q. Wang, W.H. Ko, *Modeling of touch mode capacitive sensors and diaphragms*, Sensors & Actuators 75, pp 230-241, 1999

[21] Y. Hezarjaribi, M.N. Hamidon, R.M. Sidek, S.H. Keshmiri, R.S.A. Raja Abdullah, A.R. Bahadorimehr, *Analytical and Simulation Evaluation for Diaphragm's deflection and it's applications to touch-mode MEMs Capacitive Pressure sensors,* Australian Journal of Basic and Applied Sciences, 3(4), pp 4281-4292, 2009

[22] J. Du, W.H. Ko, M. Mehregany, C.A. Zorman, *Poly-SiC Capacitive Pressure Sensors made by Wafer Bonding*, Sensors, pp 1267-1270, IEEE, 2005

[23] M.D.Giovanni, *Flat and Corrugated Diaphragm Design Handbook*, Mercel Dekker, 1982

[24] Chan, M.W., et al. *Localized Strain Sensing Using High Spatial Resolution, Highly-Sensitive MEMS Resonant Strain Gauges for Failure Prevention. Submitted to IEEE Transducers 2011.*

[25] Goericke F., et al. *High Temperature Compatible Aluminum Nitride Resonation Strain Sensor. Submitted to IEEE Transducers 2011.*

[26] Chandran, B., et al. *A Novel Bonding technique to bond CTE mismatched devices*. 1996 Proceedings 46th Electronic Components and Technology Conference, Orlando, FL, USA. pp. 1151-1158.

[27] Zhong, Z. et al. *Microstructure and mechanical properties of diffusion bonded SiC/steel joint using W/Ni interlayer*. Materials & Design. 2010.

[28] Gale, W.F. and Butts, D.A. *Transient liquid phase bonding.* Science and Technology of Welding & Joining, vol. 9 (4):283-300. 2004.

[29] Glaeser A, inventor; 1994 Dec. 13. Transient Liquid Phase Ceramic Bonding. United States patent US 5,372,298.

[30] "Phase Diagrams & Computational Thermodynamics Ag-Sn." *NIST Material Measurement Laboratory*. The National Institute of Standards and Technology (NIST). Web. <http://www.metallurgy.nist.gov/phase/solder/agsn.html>.

[31] Park, J.W. and Eagar, T.W. Application of Transient *Liquid Phase Bonding to Microelectronics and MEMS Packaging*. Advanced Packaging Materials, 2002. Proceedings. 2002 8th International Symposium on.